FRAUNHOFER SATELLITE RADIATION SENSING SYSTEMS

Stefan Metzger[a]*, Stefan Höffgen[a], Christoph Komrowski[b], Jochen Kuhnhenn[a], Tobias Kündgen[a], Michael Steffens[a]

[a] *Fraunhofer INT, Appelsgarten 2, 53879 Euskirchen, Germany*, stefan.metzger@int.fraunhofer.de, stefan.hoeffgen@int.fraunhofer.de, jochen.kuhnhenn@int.fraunhofer.de, tobias.kuendgen@int.fraunhofer.de, michael.steffens@int.fraunhofer.de
[b] *seneos GmbH, Josef-Lammerting-Allee 8, 50933 Köln, Germany*, christoph.komrowski@seneos.com
* Corresponding Author

Abstract

Fraunhofer INT develops systems for on-board radiation sensing. On-board in this context means inside electronic boxes on printed circuit boards (PCB) in close proximity to radiation sensitive electronic devices. The ability to measure dose and/or particle fluxes on the PCB is particularly of interest as this is where radiation hurts the most. In case of intense solar particle events the sudden increase of the measured particle fluxes could be used as an input for adaptive radiation mitigation techniques to protect important electronic parts and systems. Furthermore it can help to reduce radiation design margins for future missions because you get a better knowledge of the received dose inside your electronic box in a given radiation environment. In addition in the case of in-orbit verification or validation missions it is of major importance to verify the reliability of your design against the actual dose received. Our approach is to add as little devices as possible and make use of already installed hardware e.g. microprocessors to operate them, so the output of those sensor devices should already be digital. We propose to integrate additional memory devices for radiation sensing on the PCB: non-volatile UV-EPROMs to measure dose and/or SRAMs to detect high energy (solar) particles. The radiation-induced change of their digital content is a measure for the radiation exposure after calibration in a known radiation field. Fraunhofer On-board Radiation Sensors are already accepted to fly on the German geostationary Heinrich Hertz communication satellite as part of the Fraunhofer On-Board Processor and is foreseen to be implemented on-board of a NanoSat.

Keywords: Space environment; Radiation sensing; Radiation effects; Total ionizing dose; Single-event effects;

Acronyms/Abbreviations

Analog-to-digital converter (ADC), commercial off-the-shelf (COTS), device under test (DUT), Fraunhofer Institute for Technological Trend Analysis (INT), Fraunhofer On-Board Processor (FOBP), Fraunhofer On-board Radiation Sensors (FORS), geostationary orbit (GEO), Heinrich-Hertz-Satellite (H2Sat), in-orbit verification or validation (IOV), printed circuit board (PCB), silicon dioxide (SiO_2), single-event effects (SEE), single-event latch-up, single-event upset (SEU), solar particle events (SPE), static random access memory (SRAM), total ionising dose (TID), ultra-violet erasable programmable read-only memory (UV-EPROM),

1. Introduction

Currently there are several new developments and hence challenges in the space sector and satellite manufacturing like commercial and expanded use of micro and nano satellites, the use of COTS electronic components, the wish to extend the satellite life time or the application of electric propulsion for the transfer to GEO resulting in a longer passage through the radiation belts. All these changes result either in the increase of radiation exposure or the application of components or systems with reduced radiation hardness or limited knowledge of radiation tolerance.

Therefore not only the satellite manufacturers or satellite operators ask for a better knowledge of the radiation environment but also they are interested in housekeeping or health data of their system, a possibility to validate new design against a real and characterized space radiation environment and probably a support in the identification of the root cause of an in-orbit anomaly.

So INT started to develop an on-board radiation sensor system that

- is simple, robust, cheap and easy to integrate,
- measures total ionizing dose locally on the PCB,
- detects solar particle events,
- enables adaptive radiation mitigation techniques and
- supports anomaly investigation.

Our approach is to add as few devices as possible to save weight and electrical power and do not want to introduce additional causes for failures. We make use of already installed hardware e.g. microprocessors to operate them or communication channels to get the data down to Earth. This lead to the requirement that the output of those sensor devices should already be digital so that we do not need an ADC and associated electronic devices to digitize an analogue signal. Our solution is to integrate extra memory devices on the PCB: non-volatile UV-EPROMs to measure total ionising dose and/or SRAMs to detect high energy (solar) particles, especially in the case of intense SPE.

In the following section of this paper we will give details, e.g. the used sensing devices, their radiation calibration and the first implementation on the H2Sat.

2. Dosimetry with UV-EPROMs

When ionising radiation deposits energy in matter there are several consequences. At first electrons are injected from the valence bad into the conduction band where they are mobile creating electron-hole-pairs. These moving electrons are making up an electric current in accordance with field and diffusion equations. The liberated charges can be accumulated in sensitive regions or in insulating SiO_2 and can change electrical parameters, functions or states of the electrical circuits. The definition of TID is the total amount of energy absorbed in a large volume. This is the sum of all small radiation events that add an incremental amount of energy.

Each memory cell in an UV-EPROM consist of two gates: a control gate at nominal bias and an electrically isolated floating gate (see Fig. 1). The use of an UV-EPROM as a TID meter is based on the idea that ionising radiation has the same effect on the device as UV light namely removing charges (electrons) from the floating gate and the subsequent erasing of the programmed data [1].

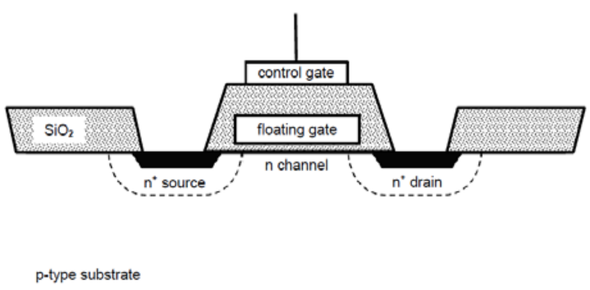

Fig. 1. UV-EPROM transistor with control and floating gate, which stores fata in form of electrons [1].

The two states of the transistor and hence of the memory cell is defined by the fact that either the floating gate is charged with electrons or left uncharged. Depending on the number of electrons on the floating gate the channel will be electrically isolating (logical “0”) or not when a read voltage is applied to the control gate. So by comparing the resulting output voltage with the decision threshold in Fig. 2 for each single cell we get a statistical distribution of “0s” and “1s”.

At the beginning, in the un-irradiated state we only have “0s”. Exposure to ionising radiation transfers energy to the electrons on the floating gate of a cell so that they can tunnel through the surrounding SiO_2 which decreases the residual number of electrons on the floating gate. With increasing dose the distribution of the cell states shifts towards the decision threshold, increasing the amount of “1s” like in Fig 2 and Fig. 3.

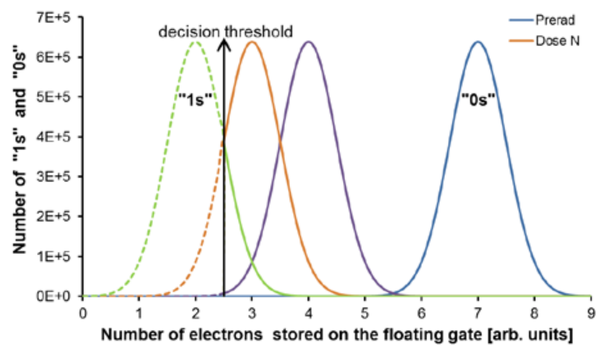

Fig. 2. Distribution of “1s” and “0s” as a function of electrons stored on the floating gate. The special form of the distribution is arbitrarily chosen.

For most of the possible distributions of the number of electrons on the floating gate we can expect that the sum of all “1s” as in Fig. 3 will have an S-shape.

So over a large range of TID the number of electrons on the floating gate and the resulting number of programmed bits is approximately proportional to the radiation exposure.

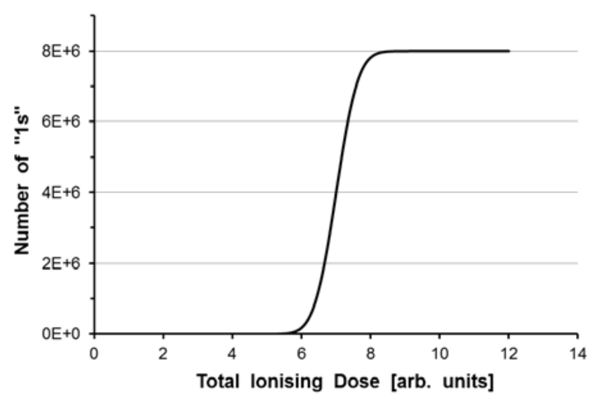

Fig. 3. Sum of “1s” (i.e. all bits that have a number of stored or residual electrons below the decision threshold in Fig. 2) as a function of received TID. Typically this curve has an “S”-shape.

It should be noted however, that the decision threshold is temperature dependent, so large variations in temperature can shift the detected number of “1s” without changing the content on the floating gates.

2.1 Used UV-EPROM

We selected an 8 Mbit (1Mb x 8) M27C801 100FG (see Fig. 4) UV EPROM from STMicroelectronics [2] because the large number of bits directly relates to the resolution of the dose measurement. The device is available in a ceramic package so that there is no outgassing problem. Although it is not of concern in our application (because we power-on the UV-EPROM only for a few seconds per hour) this family of EPROM should have some SEL immunity [3].

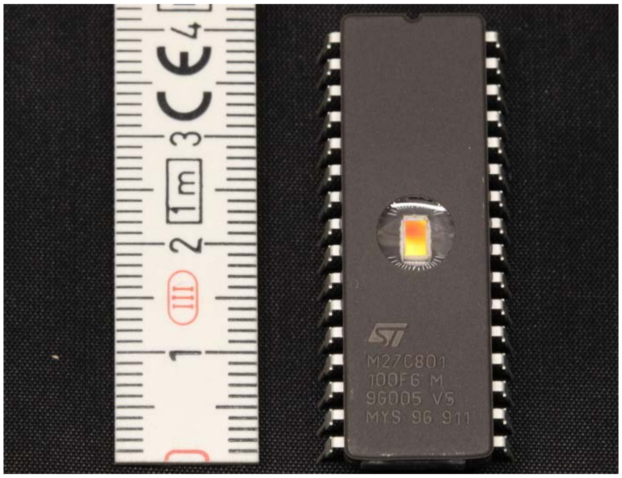

Fig. 4. Photo of the selected type of UV-EPROM for TID measurement.

2.2 Influence of external parameters on TID measurement

In order to show the ability to measure dose with these UV-EPROMs and to quantify the influence of different parameters we did a lot of different measurements. Common for all tests was that we irradiated the DUT with UV light until the first 5 to 10 % of bits were erased because otherwise we had to apply about 300 kRad(Si) until the first bits were changed from "0" to "1" and to immediately get a proportional response with TID from the device.

We only powered the UV-EPROM during reading for a few seconds and hence for most of the time, the DUTs were switched off resulting in increased radiation hardness, similar to the on-board measurement procedure. The exact duty-cycle will be defined for each mission accordingly, but we propose not to go below 1:100 so that the exposure while the UV-EPROM are powered on remains well below 10 kRad(Si) over the mission.

During the characterisation measurements we always hold all but one parameter constant. We checked the sensitivity of the UV EPROM to changes of the following external factors:

- reproducibility of dose measurement with the same device
- device to device variability
- dose-rate dependence
- temperature effects
- supply voltages (during read or write)
- programming voltage and duration

In the following Fig.5 the influence of dose-rate during Co-60 gamma irradiation on the erasing behaviour is presented for 3 different devices. Here 5 % of the programmed "0s" were erased to "1s" with UV-light before starting the gamma irradiation. We see the typical S-shape curve with a maximum usable range of ca. 100 kRad(Si) (left side is truncated due to the pre-erasure with UV-light). After the LDR-irradiation sequence the same DUTs were fully re-programmed and pre-erased to 5 % with UV-light and re-irradiated at high dose-rate with Co-60 gammas.

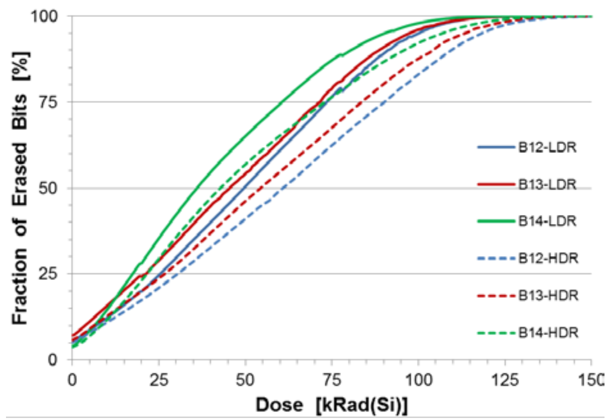

Fig. 5. Successive TID measurements with the 3 different device (B12, B13 and B14) during Co-60 gamma irradiation at 0.27 kRad(Si)/h (= LDR, solid lines) and 2.9 kRad(Si)/h (= HDR, dashed lines).

In Fig. 6 the best suited range for TID measurement is shown for 2 devices (B12 and B13). This is the fraction between 20 and 80 % of erased bit corresponding to a dose range of approx. 60 kRad(Si). There we will have the highest sensitivity (derivative or slope) and the curve is nearly a straight line. This linear behaviour is an advantage for our application because it guarantees that those 60 % of all UV-EPROM cells (i.e. those between 20 and 80 %) nearly have the same sensitivity to Co-60 gammas because they are programmed to the more or less the same electron content on the floating gate before. In addition this makes the TID measurement more robust against variations of the decision threshold due to external influences like changes of temperature, supply voltage as long as we measure the number of erased bits always at the same operating conditions.

The device-to-device variation which is about 10 % of the erased bits is not a real concern in our approach because we will measure the TID response for every flight dose meter (= UV-EPROM) once before start and get directly its sensitivity.

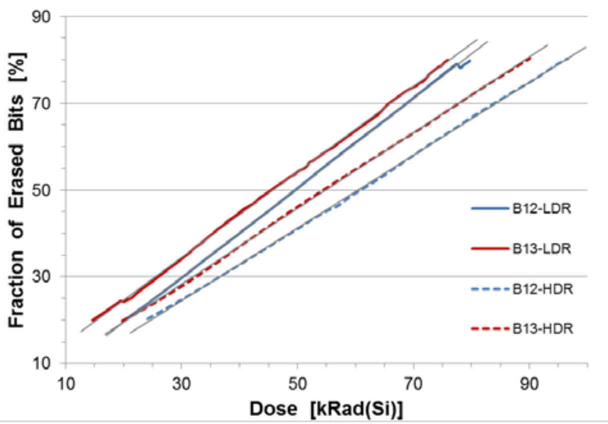

Fig. 6. Best suited measurement range between 20 and 80 % of erased bits for the 3 devices B12 and B13. The straight lines (thin grey solid lines) are only to guide the eye.

In the end we came up with a set of standard external parameters. Those and their influence on the dose measurement are presented in Table 1. The column "influence" means the change in the number of flipped bits when the parameter is changed as given in Table 1, e.g. when the supply voltage during read is changed from 5 to 5.1 V the number of flipped bits changes 10 %. Most of these effects are due to the decision threshold rather than the physical state of the individual floating gates.

Table 1. Nominal values for important external parameters and their influence on the number of flipped bits [4].

parameter	nominal value	influence
supply voltage during read	5 V	+/- 10 % per 0.1 V
supply voltage during programming	6.5 V	+/- 10 % per 1 V
programming voltage	12.75 V	+/- 20 % per 1 V
programming time	50 µs	+/- 10 % per 10 µs
temperature during read	mission dependent	+/- 1 % per 5 K

3. Proton flux measurement through counting of SEUs in a CMOS SRAM

3.1 Principle of SEU measurement

When heavy charged particles, e.g. iron nuclei from the galactic cosmic radiation, hit a semiconductor device they produce densely ionised regions of electron-hole pairs along their tracks. In the case of protons or neutrons secondary particles (e.g. silicon recoils) produced in nuclear reaction are the source for the following ionisation. The produced electrons are swept away and collected by electric fields in the depletion regions of transistors in the off-state (non-conducting) (see Fig. 7). If the amount of collected charges is greater than a critical number (i.e. the threshold charge) an effect is induced in the semiconductor device. The effects can either be temporal and reversible such as changing the information in a memory cell or permanent and destructive like a burnout in a power device. In the case of a static CMOS RAM we have to expect two types of SEE: firstly a SEU (see Fig. 7) where the information is changed from "1" to "0" or vice versa and secondly a SEL, which is in our case negligible because the type we selected is latch-up free [5].

If in Fig. 8 the PMOS transistor in the off-state is hit, the voltage difference between source and drain is reduced below V_{DD}. If the voltage drop on the output of inverter no. 1 is long enough below the threshold of the input of inverter no. 2 (i.e. cross-coupling over the feed-back loop) the bitflip is locked into the SRAM cell.

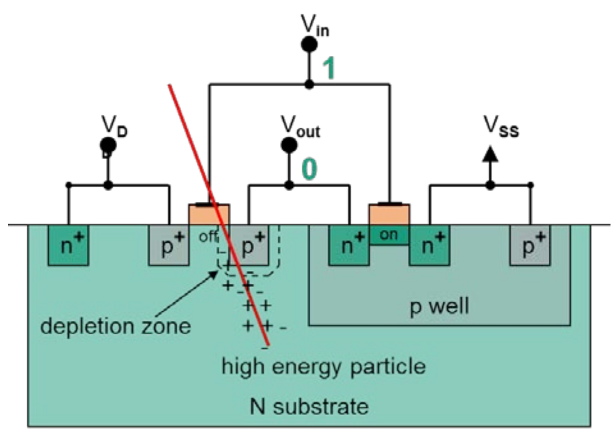

Fig. 7. High energy heavy particle hitting a CMOS inverter, producing a dense track of ionisation.

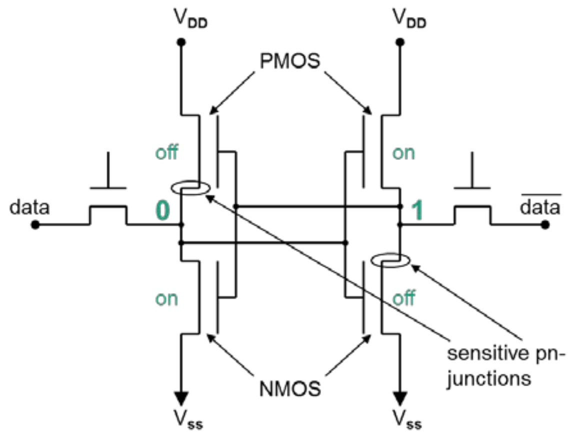

Fig. 8. Sketch of a 6-transistor CMOS SRAM cell, consisting of two cross-coupled inverters. In each inverter one transistor is conducting (on-state) and one is blocked (off-state).

3.2 Used type of CMOS SRAM

We have chosen a 4 Mbit SRAM 5962-0520804VYC in QML-V quality which is based on AT60142H (see Fig. 9) from Atmel [5, 6] due to several reasons: 1) it is a low power static RAM, 2) it is produced on a radiation hard CMOS process and 3) it is commonly used in the space community as a particle detector in the ESA SEU monitor and also used on-board of the PROBA II satellite [7]. In particular the last two reasons are of importance because those SRAMs are tested up to a total dose of 300 kRad(Si) and are SEL free up to a threshold of 80 MeV/mg/cm^2 (at 125 °C) [5]. And there exist a large data base of calibration data for the SEU sensitivity of this device type.

Fig. 9. Photo of the selected type of SRAM for the detection of solar particles.

3.3 Calibration of the CMOS SRAM

Fortunately this type of CMOS SRAM was already calibrated at several proton facilities [7] so that the SEU sensitivity as a function of proton energy is well known (see Fig. 10) and can be used for our application. In addition the heavy ion SEU cross section is known so that we are able to calculate the SEU background rate due to galactic cosmic rays.

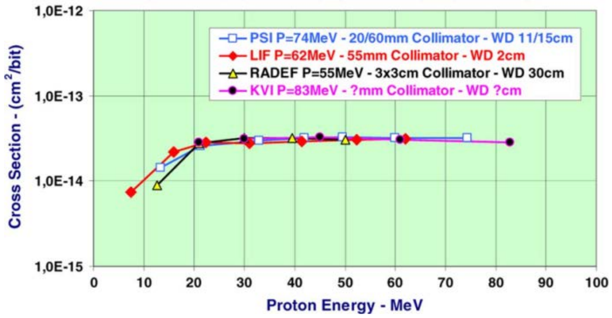

Fig. 10. Proton calibration data from four different facilities [7].

4. Implementation into the FOBP on H2Sat

The H2Sat is a geostationary communication satellite based on OHB's Small GEO platform under a contract from the German space agency DLR. It foreseen to be launched in 2021 or 2022. The goals of H2Sat are to show German competences in building communication satellites and to verify or validate new communication techniques in orbit [8]. Among those the Fraunhofer Society represented by its Fraunhofer institute IIS has an accepted payload called the FOBP [9]. The principal design approach is shown in Fig.11. We make use of all existing electronic parts and subsystems of the FOBP and only add two distinct memory devices, i.e. one UV-EPROM for TID measurement and one SRAM for detection of high energy particles. The FOBP will get dedicated measurement slots during the mission and will only be operational during those times. Hence the SEU monitor can only detect particles through SEU counting during those time slots but luckily the UV-EPROM is able to measure the integral dose offline. So it isn't affected by the FOBP downtimes.

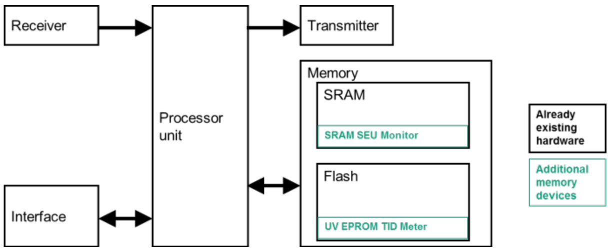

Fig. 11. Implementation of the FORS system into the FOBP.

In Fig. 12 a photo of the processor board is presented. We are in closed proximity (ca. 15 cm) away from the core of the FOBP and so we can produce a precise value for the dose and number of particles impinging on the FOBP. It also gives an impression of the thickness of the surrounding walls of the box. This will be including the outer walls of the satellite an equivalent of 7 mm Aluminium.

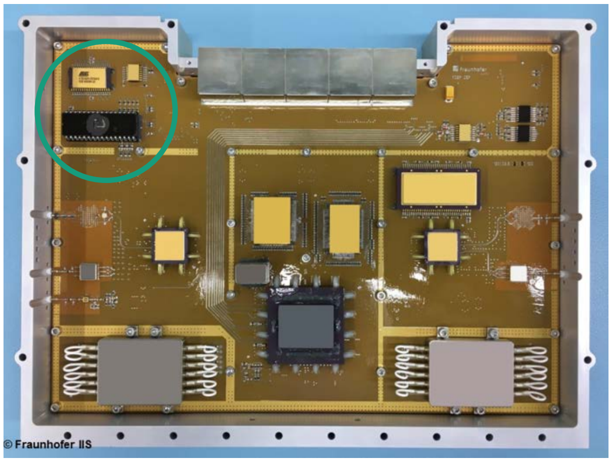

Fig. 12. Photo of the processor board inside the FOBP with the two memory devices (inside the green circle) making up the FORS (© Fraunhofer IIS).

4.1 Expected environment (TID, SPE)

Inside the FOBP on-board of H2Sat we have to calculate with an equivalent thickness of 7 mm Al.

The dose depth curve in Fig. 13 is from the original mission planning of about 14 days in geo transfer followed by an operational lifetime of 15 years in GEO [10]. According to this we would have to expect a total mission dose of about 21 kRad(Si) behind 7 mm Al equivalent shielding. As of now it is most likely that the transfer will be accomplished by electric orbit raising and so we might encounter up to 50 % extra dose [11], which will be about 30 kRad(Si). This is a factor of two below the best suited 20 to 80 % range of the fraction of flipped bits in e.g. Fig. 6. and so we expect sufficient margin for additional TID measurement.

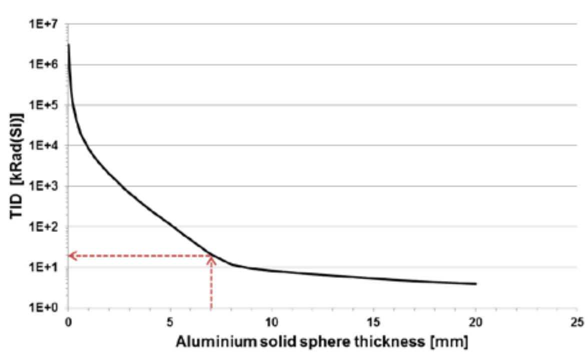

Fig. 13. Dose depth curve inside a solid Al sphere for the H2Sat mission according to [10].

For the H2Sat mission we will calibrate the flight model of the UV-EPROM (and hence any sensor that would fly on any other mission) individually under standard conditions like dose-rate, temperature before delivering it to IIS and integration into their FOBP.

Based on the proton fluxes in the expected radiation environment given in [10] we expect ca. 0.1 SEU per day during quiet conditions. This is our SEU background rate. During a large SPE like those depicted in Fig. 14 we have to deal with total proton fluences between 10^9 and a few times 10^{10} protons/cm^2 [12]. As the protons lose about 40 MeV while penetrating 7 mm Al [13] (i.e. $E_{min,1}$ in Fig. 14) and adding another 20 MeV for reaching the saturation cross section in Fig. 10 (i.e. $E_{min,2}$) we can expect a relevant proton fluence with energies greater than 60 MeV between 10^8 and several 10^9 protons/cm^2 that are able to induce SEUs in the SRAM behind 7 mm of Al. So we estimate between a few tens and several hundreds of SEUs in total during solar storm conditions (within several hours).

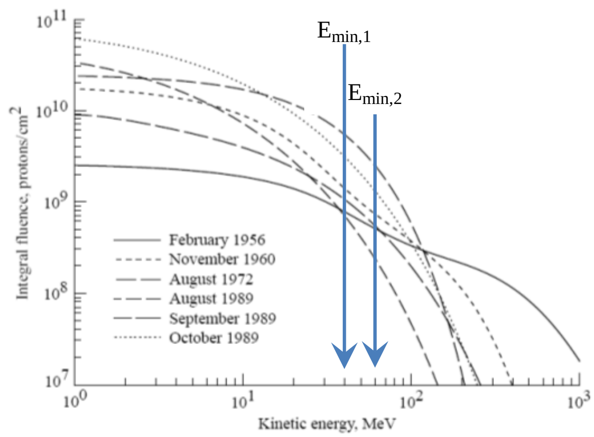

Fig. 14. Solar proton event fluence spectra for several large solar events [11]. $E_{min,1}$ and $E_{min,2}$ are explained in the text.

5. Conclusions

In our FORS approach of on-board radiation sensing we are able to independently measure TID and solar protons. TID sensing is done with an UV-EPROM where the applied dose is proportional to the number of flipped bits, working as a integrating dose meter even when it is unpowered. Whereas the high energy protons are detected through counting the number of induced bit-flips in a static RAM during operation. A first system will fly on the German H2Sat in 2021.

References

[1] L. Scheick, P.J. McNulty, D.R. Roth, Dosimetry Based on the Erasure of Floating Gates in the

Natural Radiation Environments in Space, IEEE Trans. Nucl. Sci, 45 (1998) 2681-2688.

[2] STMicroelectronics, M27C801, data sheet revision no. 6, September 2007.

[3] HIREX Engineering, Heavy Ion Single Event Effects Radiation Test Report – Part Type M27C512, ESA_QCA0414S_C Report issue no. 1, September 2004.

[4] C. Komrowski, Charakterisierung von UV-EPROMs mit einem erstellten Lese- und Schreibmodul, Masterthesis, University of Applied Sciences Koblenz, August 2017.

[5] Standard microcircuit drawing, 5962-05208 revision C, April 1997.

[6] ATMEL, AT60142H, data sheet revision B, May 2010.

[7] R. Harboe-Sørensen, C. Poivey, Member, F.X. Guerre, A. Roseng, F. Lochon, G. Berger, W. Hajdas, A. Virtanen, H. Kettunen, S. Duzellier, From the Reference SEU Monitor to the Technology Demonstration Module On-Board PROBA-II, IEEE Trans. Nucl. Sci. 55 (2008) 3082-3087.

[8] S. Voigt, The German Heinrich Hertz Satellite Mission, 2010 Proceedings of the Fourth European Conference on Antennas and Propagation (EuCAP), April 2010 1-4.

[9] A. Hofmann, R. Wansch, R. Glein, B. Kollmannthaler, An FPGA based On-Board Processor Platform for Space Application, in NASA/ESA Conference on Adaptive Hardware and Systems (AHS), June 2012 17–22.

[10] OHB Systems, General Equipment Requirements Document (GERD) for the Small GEO Satellite, TC-OHB-RQ-0001, Issue 02, Rev. A, 27.09.2011.

[11] R.B. Horne, D. Pitchford, Space Weather Concerns for All-Electric Propulsion Satellites, Space Weather 13, doi:10.1002/2015SW001198.

[12] J.W. Wilson, J.L. Shinn, L.C. Simonsen, F.A. Cucinotta, R.R. Dubey, W.R. Jordan, T.D. Jones, C.K. Chang, M.Y. Kim, Exposures to Solar Particle Events in Deep Space Missions, NASA Technical Paper 3668, October 1997.

[13] Atomic Data and Nuclear Data Tables, Part 2 Elements, Volume 27, nos. 4/5, July/September 1982.